Exploring and tuning the anchorage of chlorophyllin molecules on anionic clays

CrossMark

Alicia Sommer[a], Aldo Romero[a], Geolar Fetter[a,*], Eduardo Palomares[b], Pedro Bosch[c]

[a] Universidad Autónoma de Puebla, Facultad de Ciencias Químicas, 72570 Puebla, PUE, Mexico
[b] Universidad Politécnica de Valencia, Instituto de Tecnología Química (UPV-CSIC), 46022 Valencia, Spain
[c] Universidad Nacional Autónoma de México, Instituto de Investigaciones en Materiales, 04510 México, D.F., Mexico

ARTICLE INFO

ABSTRACT

In experiments modeling photosynthesis, well dispersed chlorophyll molecules are required. A solution could be to anchor them on some host. In this work, new hybrid materials are synthesized using hydrotalcite and a chlorophyll derivative: chlorophyllin. Chlorophyllin is incorporated and dispersed in hydrotalcite through simultaneous precipitation or during hydrotalcite reconstruction. The effect of microwave irradiation on the crystallization step is discussed. In all cases stable materials are obtained, chlorophyllin molecules are isolated and bonded through hydrotalcite OH groups.

© 2013 Elsevier B.V. All rights reserved.

1. Introduction

Green plants, algae, and cyanobacteria use the energy from the sun through well dispersed chlorophyll molecules. Indeed, chlorophyll is the principal photoreceptor in photosynthesis as it acts as a light collector. In fact, the function of the vast majority of chlorophyll (up to several hundred molecules per photosystem) is to absorb light and transfer that light energy to a specific chlorophyll pair in the reaction center of the photosystems. Due to the chlorophyll selectivity regarding the wavelength of light it absorbs, leaves containing the molecule will appear green. In green leaves, chlorophyll molecules bind to proteins to form chlorophyll–protein conjugates in which the chlorophyll interaction plays an important role in physiological functions and stabilization of plant leaves [1].

Natural chlorophyll extracted from living leaves has been seldom used in artificial photosynthesis because of its instability as a pigment, as a dye, or as a molecule. Once extracted with a solvent (such as acetone or methanol), the chlorophyll pigments can be separated in a simple paper chromatography experiment [2]. Based on the number of polar groups, several chlorophyll molecules

may be distinguished: *a*, *b*, *c* (1 or 2) or *d*. When leaves degreen in the process of plant senescence, chlorophyll is converted to a group of colorless tetrapyrroles known as nonfluorescent chlorophyll catabolites [3].

Chlorophyll may be stabilized using an inorganic support. Itoh et al. [4] have demonstrated the importance of chlorophyll–support interactions, adsorbing chlorophyll *a* on silicate layers of smectite. The resulting hybrid material shows photostable and photocatalyzing properties. The interaction is such that acid-activated montmorillonite clay is the industrial standard for removing chlorophyll, carotenoids, or phospholipids, among other products, from oils. This application has remained unchallenged, since its introduction at the beginning of this century; it is also fair to say that a complete understanding of the reasons for its dominance (over other clay minerals) is still lacking. This is true in spite of numerous studies relating the role of various physical/chemical properties of acid-activated clays to their pigment adsorption efficiencies [5,6]. Then, the retained chlorophyll could be used as a photocatalyst or in any other process involving photosynthesis. However, smectites are acidic clays which may degrade chlorophyll through a substitution process. To avoid such degradation semi-synthetic derivatives of chlorophyll, differing in the identity of the cations associated with the complex anion have been commercialized, among them chlorophyllin.

Chlorophyllin is the active ingredient in a large number of internally taken preparations intended to reduce odors associated with incontinence, colostomies, and similar procedures, as well as body
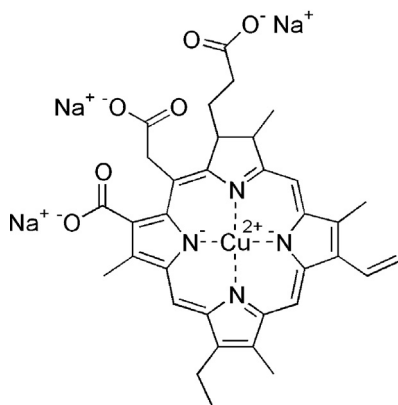
Fig. 1. Trisodium copper chlorophyllin structural formula.

odor in general. It is also used in the treatment of wounds, injuries, and other skin conditions, notably radiation burns. Moreover, chlorophyllin may be found in food additives and in alternative medicine [7]. The most common form is a sodium/copper derivative of chlorophyllin, Fig. 1. Although it is present in green leafy vegetables, it reaches at most only 5.7%. Unlike natural chlorophyll, chlorophyllin is water-soluble.

As chlorophyllin can be described as an anionic species, clays with basic properties, *i.e.*, with anion exchange sites, could favor, on the one hand, the stabilization of chlorophyllin and, on the other hand, the dispersion of the molecules. In this sense, the proposed chlorophyllin–hydrotalcite hybrid compound should present original features which guarantee new applications.

Hydrotalcites are layered compounds with anionic exchanger properties [8]. Hydrotalcites have as general formula:

$$[M_{1-x}^{2+}M^{3}+x(OH)_2](A^{m-})_{x/m} \cdot nH_2O$$
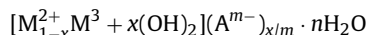
where M^{2+} is a divalent metal that may be replaced by a trivalent atom, M^{3+}, which produces positively charged layers. This charge is neutralized by A, a compensating anion with charge $m-$ as CO_3^{2-} or NO_3^{-}; x represents the metal ratio $M^{3+}/(M^{3+} + M^{2+})$, and n is the number of crystallization water molecules. Hydrotalcite properties are determined by the nature of the cations, the ratio M^{3+}/M^{2+}, the synthesis method, among others [8,9]. Hydrotalcites may be expanded introducing compounds between the layers, the process is known as intercalation and it is generally used to increase the porosity of these materials [9]. In some cases, the intercalation or structural modification is obtained through the regeneration of the double layered hydroxide structure, *i.e.*, the "memory effect", which is a characteristic feature of these materials [10]. Intercalated hydrotalcites are often used as drug deliverers [11]. Hydrotalcite is not toxic and it is often recommended as a stomach antiacid [12]. Therefore, chlorophyllin–hydrotalcite conjugates should present several advantages: stability, strong interaction between chlorophyllin and the hydrotalcite layers, dispersion of the organic molecules into the inorganic matrix.

In this work, we report, for the first time, on the chlorophyllin retention in hydrotalcites. The samples were obtained through two methods: memory effect (reconstruction of the hydrotalcite structure from mixed oxides using chlorophyllin as anion) or simultaneous synthesis (coprecipitation of hydrotalcite in presence of chlorophyllin). Considering the various advantages of microwave irradiation during the crystallization step, such as the reduction of the synthesis time, or a better diffusion and distribution of the intercalated species [13], microwave irradiation should direct the insertion of chlorophyllin.

2. Experimental

2.1. Synthesis

2.1.1. Materials

Aluminum and magnesium nitrate, both from Sigma–Aldrich (98% and 99% purity), were used as reactants to synthesize hydrotalcite. Sodium hydroxide (Baker, 99.5% purity) was the precipitating agent. Chlorophyllin (98% purity) was provided by Natural Health.

2.1.2. Samples

2.1.2.1. *(a) Synthesis through memory effect.* The REF sample, Mg/Al hydrotalcite-like sample, was synthesized from a Mg- and Al-nitrate aqueous solution (2.5 M) and a sodium hydroxide solution (1.88 M). The flow of each solution was adjusted to maintain a constant pH of 11. The amounts correspond to a molar ratio Mg/Al of 3. The resulting gel was treated in a microwave autoclave (MIC-I Sistemas y Equipos de Vidrio S.A. de C.V.) for 10 min operating at 2.45 GHz. The microwave equipment consists of a glass reactor of 500 mL, which fits in a microwave oven whose power may be selected. A stirring mechanism is adapted to the reactor so that temperature is the same all over and it is controlled through an infrared radiation sensor. Temperature was fixed at 80 °C and power at 200 W. The solid was recovered by decantation and washed with distilled water up to a pH value of 10 and dried in an oven at 70 °C. The hydrotalcite was calcined at 500 °C for 4.5 h and 1 g of the resulting oxides was dispersed with distilled water under stirring. Then, NaOH 1.88 M (19.25 mL) was added. Chlorophyllin (3.65 mL), as provided, was dropped into this mixture and stirred for 10 min. The obtained slurry was treated at 80 °C for 12 h (crystallization step) in a reactor connected to a condenser and heated by a blanket system. The solids were recovered by decantation and washed several times until the pH value of the waste water was 10.7. The sample was, then, dried at 70 °C for 24 h, sample R-OHCV. A second sample containing chlorophyllin was prepared in the same conditions but dispersing the oxides in water and not adding NaOH, sample R-CV.

Another set of samples was prepared in presence of microwave irradiation. Sample R-OHMW corresponds to sample R-OHCV treated with microwave irradiation (200 W, 10 min, 80 °C) during the crystallization step, *i.e.*, after chlorophyllin addition. Sample R-MW corresponds to sample R-CV but microwave irradiated after chlorophyllin addition in the same conditions as previously.

2.1.2.2. *(b) Simultaneous precipitation.* Three samples were prepared, one by crystallization in a conventional reactor and the two others in presence of microwave irradiation. The first sample was synthesized as follows. A solution containing magnesium and aluminum nitrates (2.5 M) was mixed with a sodium hydroxide solution (1.88 M) and dropped onto the chlorophyllin initially deposited in the reactor at constant pH of 11. The slurry was treated at 80 °C for 12 h. The solids were recovered by decantation and washed several times until the waste water pH reached 9.3 and, then, they were dried at 70 °C for 24 h, sample B-OHCV.

The second sample was synthesized as the previous one but the crystallization step was carried out under microwave irradiation in the same conditions.

In the last sample, chlorophyllin and hydrotalcite precursors were dropped simultaneously, sample S-OHMW. The labeling of the chlorophyllin containing samples is summarized in Table 1.

Table 1
Synthesis conditions of the samples.

Synthesis method	Hydrotreatment	Precipitating agent	Sample
Memory effect	Conventional	NaOH	R-OHCV
		–	R-CV
	Microwave	NaOH	R-OHMW
		–	R-MW
Simultaneous precipitation	Conventional	NaOH	B-OHCV
	Microwave	NaOH	B-OHMW (HT precursors dropped over chlorophyllin)
			S-OHMW (Chlorophyllin and HT precursors mixed)

2.2. Characterization methods

2.2.1. CHNS-O elemental analyzer

A Fisons EA-1108 CHNS-O elemental analyzer was employed to determine the N, C and H contents of the samples.

2.2.2. Inductively coupled plasma (ICP)

The Al, Mg and Cu content was measured by ICP-OES. The samples (*ca.* 20 mg), previously calcined, were dissolved in a HNO_3/HCl (1/3 vol.) solution before analysis in a Varian 715-ES ICP-Optical Emission Spectrometer.

2.2.3. X-ray diffraction

A Bruker-axs D8-advance diffractometer coupled to a copper anode X-ray tube was used to identify the compounds present in the powdered samples. A diffracted beam monochromator selected the Kα radiation.

2.2.4. FTIR spectroscopy

FTIR spectra in the region $4000-400\ cm^{-1}$ were obtained with a Magna-IR Spectrometer 550 Nicolet. The pellets were prepared with KBr.

2.2.5. Nitrogen adsorption

The BET surface areas were determined from the nitrogen adsorption-desorption curves by the conventional multipoint technique with a Micromeritics ASAP 2020. The pore size distribution curves were obtained applying the BJH method to the desorption branch. The samples were pretreated at 150 °C for 12 h at high vacuum.

2.2.6. Thermal analysis

Thermogravimetry and differential thermal analyses were obtained, under air flow ($50\ cm^3/min$), using a Mettler Toledo TGA/SDTA 851 equipment. The sample weight was about 10 mg. The experiments were carried out in the range 25–800 °C with a heating rate of 10 °C/min.

2.2.7. UV–vis and DR-UV spectroscopy

For liquid chlorophyllin UV–vis (visible ultraviolet) was used but for the presented hybrid materials the technique was DR-UV (diffuse reflectance ultraviolet). A Varian Cary 5000 UV–vis-NIR spectrophotometer was used at 600 nm/min. The scanning was from 200 to 800 nm.
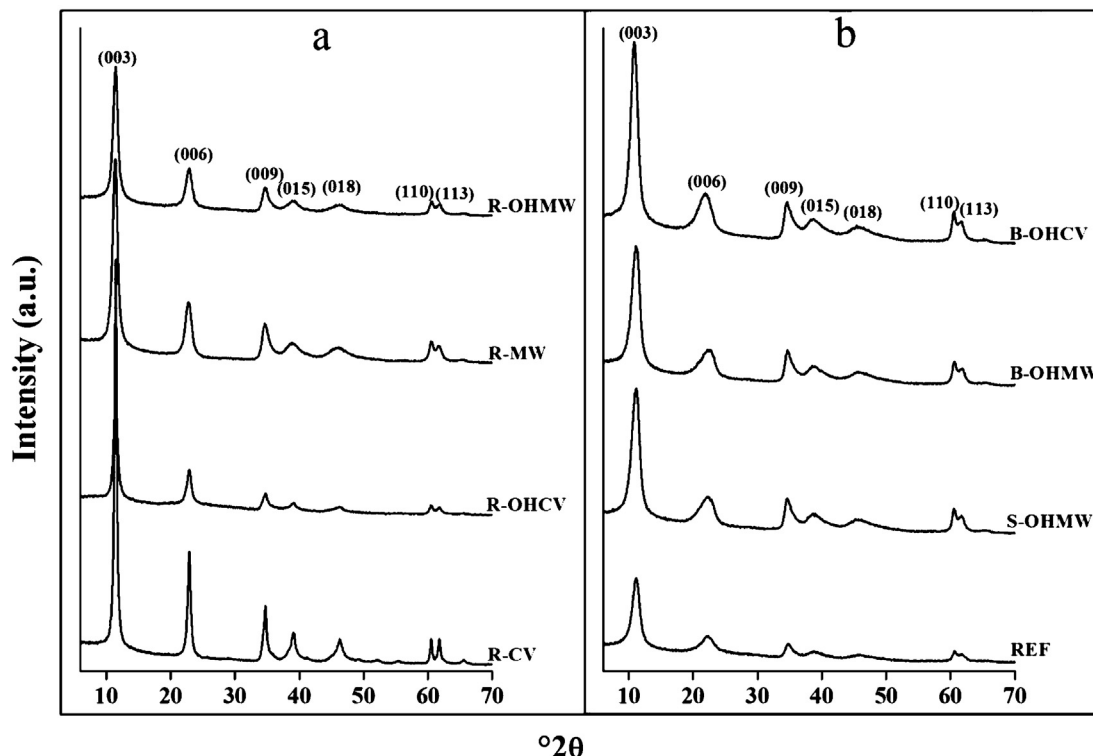

Fig. 2. X-ray diffraction patterns of samples (a) synthesized by memory effect or (b) simultaneous precipitation methods.

Table 2
Comparison of the sample elemental composition. Mg, Al and Cu amounts were determined by ICP-OES whereas N, C and H contents with a CHNS/O elemental analyzer.

Sample	Mg/Al molar	Cu/Al molar ($\times 10^{-4}$)	C (mol/g)	N (mol/g)
R-OHCV	3.4	36.4	0.23	0.02
R-CV	3.3	6.95	0.22	0.04
R-OHMW	3.2	6.99	0.18	0.07
R-MW	3.1	5.93	0.17	0.09
B-OHCV	3.1	23.9	0.12	0.21
B-OHMW	3.0	24.9	0.14	0.18
S-OHMW	3.0	23.6	0.13	0.19
REF	3.1	0	0.07	0.19

3. Results

3.1. Compounds

The diffractograms are compared in Fig. 2; all samples are crystalline and are identified as hydrotalcite. The first X-ray diffraction peak of samples synthesized through regeneration (labeled R-) is located at $d_{003} = 7.7$ Å. Instead, in those synthesized by simultaneous precipitation (labeled B- or S-) it is equal to 8.1 Å.

When $d_{003} = 7.7$ Å, the interlayer space is 2.9 Å, that corresponds a layer thickness 4.8 Å. This value corresponds to hydrotalcites interlayered with carbonates whose size is *ca.* 3.0 Å. Then, chlorophyllin must be intercalated parallel to the hydrotalcite layers as chlorophyllin molecular size, estimated from the bond lengths, is 2.7 Å × 7.1 Å × 10.3 Å.

When $d_{003} = 8.1$ Å, the interlayer space turns out to be 3.3 Å, then, the space is determined mainly by nitrates and carbonates. In this case, again, chlorophyllin may be intercalated. Note that the samples are all green and that no other crystalline compounds than hydrotalcite are identified.

3.2. Elemental composition

In the regenerated samples copper content turns out to be 12.1×10^{-4}, 2.39×10^{-4}, 2.30×10^{-4}, and 2.04×10^{-4} mol/g, in samples R-OHCV, R-CV, R-OHMW, and R-MW, respectively. Copper content reveals the chlorophyllin presence. Chlorophyllin content of sample R-OHCV is almost six times greater than the others, whose retention is close to 2.4×10^{-4} mol/g. Table 2 shows that the relative amount of exchange sites, due to the substitution of magnesium by aluminum, varies between a molar ratio Mg/Al of 3.1 and 3.4. As the experimental molar ratio Mg/Al is closer to the nominal value of 3 in the microwave irradiated samples, irradiation propitiates the incorporation of aluminum into the hydrotalcite network.

These sites may be occupied by carbonates or chlorophyllin. In the REF sample, the amount of nitrogen (0.19 mol/g) and carbon (0.07 mol/g) are due to the interlayered anions (carbonates and nitrates). The nitrogen amount in the chlorophyllin containing samples (0.02–0.09 mol/g) is attributed to the nitrogen content of the chlorophyllin which is expected to block the exchange sites in the hydrotalcite layers, as shown by the molar ratio Cu/Al.

Again, as the elemental composition of samples R-OHMW and R-MW is similar, one could conclude that the presence of OH during the synthesis is not relevant. Instead, samples R-OHCV and R-CV show that OH ions promote chlorophyllin retention. Thus, microwave irradiation alters the preference sequence of the hydrotalcite as it favors the diffusion of the smaller ions (carbonates and hydroxyls) [14], inhibiting the chlorophyllin intercalation.

When the hydrotalcite promoters (NaOH and Mg- and Al-nitrate aqueous solutions) are dropped on a chlorophyllin solution, or mixed simultaneously, the resulting compound is a hydrotalcite
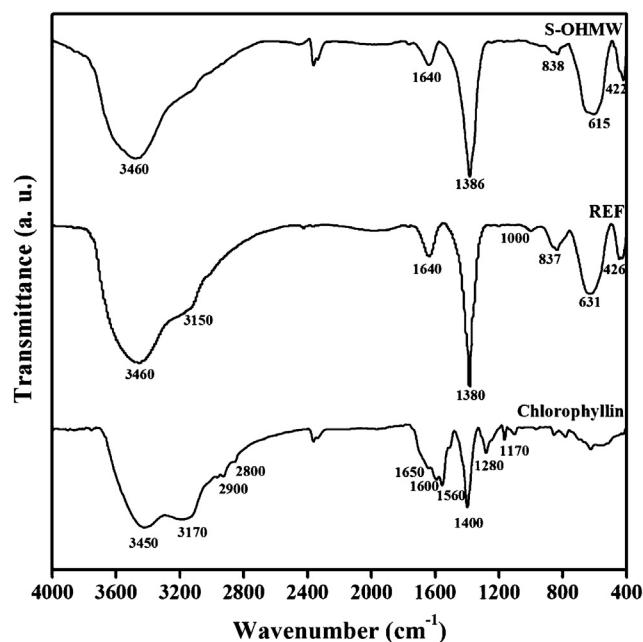

Fig. 3. Infrared spectra of the chlorophyllin, REF and S-OHMW samples.

(samples B-OHCV, B-OHMW and S-OHMW) with a nitrogen content (0.21, 0.18, 0.19 mol/g) close to 0.19 mol/g which is the value found for the REF sample. Indeed, a main difference between these and the regenerated samples is the presence of nitrates, in the reaction slurry, prone to be intercalated in the resulting hydrotalcite. It is not surprising that the interlayered anions are mostly nitrates. Chlorophyllin is, then, expected to be retained at the outside charged centers, as pore mouths or defects, the molar ratio Cu/Al is comprised between 23.6×10^{-4} and 24.9×10^{-4}, Table 2. As nitrates are small ions with a high mobility they compete advantageously with chlorophyllin and they occupy most of the internal exchange sites. The simultaneously precipitated sample, in presence of microwaves, S-OHMW, shows an intermediary composition of carbon and nitrogen between the B-OHCV and B-OHMW. Note that samples R-OHCV and B-OHCV differ in their nitrogen content which is 0.02 and 0.21 mol/g, respectively, then the first one has incorporated chlorophyllin between the layers to compensate the charges and the second one has chlorophyllin distributed all around as previously discussed.

3.3. Infrared spectroscopy

In the chlorophyllin spectrum, Fig. 3, the bands at 2800–3450 cm^{-1} and 1350–1450 cm^{-1} correspond to CH$_2$—CH$_2$ groups. The bands appearing at 1500–1700 cm^{-1} are due to C=N—C groups. The small and broad bands at 1650 – 1750 cm^{-1} can be attributed to ester radicals (H—CO—O—R) [15].

In the hydrotalcite spectra, REF, the absorption band at 3460 cm^{-1} is attributed to OH stretching vibrations in the lamellae. The angular deformation, due to water OH groups, appears at 1640 cm^{-1}. The band at *ca.* 1380 cm^{-1} corresponds to the overlapping bands of nitrates and carbonates. The bands comprised between 420 and 833 cm^{-1} are related to Mg—O and Al—O vibrations [16,17].

The REF and all other chlorophyllin containing samples spectra are similar, then, only the S-OHMW spectrum is shown in Fig. 3. As the chlorophyllin bands overlap those of hydrotalcite (REF sample), it was not possible to determine the presence of chlorophyllin by FTIR. However, the partial intercalation of carbonates and nitrates (1380 cm^{-1}) is confirmed.

3.4. Nitrogen adsorption

R-OHCV and R-CV isotherms correspond to a Type IV in the IUPAC classification, Fig. 4. The hysteresis profiles are H1 type (IUPAC), characteristic of slit shaped mesopores, often present in lamellar materials [18–20], open in both extremes and with a pore size distribution characterized by a peak at 30 Å and a second one found at 95 Å in sample R-OHCV and 50 Å in R-CV, Fig. 5. The corresponding specific surface areas are 76 and 61 m^2/g. The pore size distribution of the REF sample has also two peaks, one at 30 Å and the other at 50 Å. In this sample the pores are as well slit shaped, Table 3.

Instead, the microwave regenerated samples (R-OHMW and R-MW) present a type IV isotherm but a H3 hysteresis loop corresponding to ink bottle shaped pores [21], such pores are, of course, inter-particle pores. On the one hand, the pore size distribution of sample R-OHMW presents two peaks, one at 30 Å and the other hand at 60 Å; on the other, pore size distribution of R-MW has a peak at a diameter of 30 Å and a very broad peak from 50 to 300 Å. Such profile has to be interpreted as due to a house of cards structured material. The corresponding surface areas are 39 and 27 m^2/g. The addition of OH during the regeneration process promotes a higher surface area in 20–30%.

The isotherms of the samples B-OHCV, B-OHMW and S-OHMW present isotherms type IV, *i.e.*, they are mesoporous. The B-OHCV sample has slit shaped pores as the hysteresis loop is H1. Instead, the pores of the other two samples are ink bottle shaped (hysteresis loop H3). The pore size distribution is similar in these three samples as it shows maxima for diameters of 30 and 50 Å, but in samples S-OHMW and B-OHMW the distributions are very broad. The specific surface areas are 17 m^2/g (B-OHCV), 10 m^2/g (B-OHMW) and 11 m^2/g (S-OHMW). Microwave irradiation produces materials with a small specific surface area and deep green color.

3.5. Thermal analysis

The thermal gravimetric analysis curves of samples R-OHCV and R-CV are similar, Fig. 6. The curves may be divided in three stages: the first one (weight loss of 14%) from 25 to 240 °C corresponds to water loss [16,22]; the second one (25 wt.%) from 240 to 450 °C may be attributed to carbonates and chlorophyllin decomposition; the third one ends up at 800 °C at a lower rate (4 wt.%) [23]. Samples R-MW and R-OHMW are again similar, the only differences from the previous samples is that during the first stage the weight loss is only 9%, and that the second stage begins at 220 °C and finishes at 400 °C.

When the thermal behavior of B-OHCV, B-OHMW and S-OHMW samples is compared, in the first stage (from 25 to 140 °C) the weight loss is 12%. In the second stage (from 140 to 400 °C) the weight loss turns out to be again 25%, but the broad centered peak (DTA) at 390 °C is now resolved. A first maximum appears at 390 °C, a second one at 410 °C and the last one at 440 °C, whose relative intensities are variable. Of course, these differences have to be attributed to the strength of the chlorophyllin–support interaction.

The REF sample liberates at 390 °C water, nitrate, and carbonate, which are endothermal processes. Instead, chlorophyllin presents two endothermic peaks at around 170 °C and 280 °C, followed by a broad exothermic peak at around 440 °C, which correspond, respectively, to the evaporation of water, the Cu ion elimination from the chlorophyllin structure, and the degradation of the chlorophyllin structure [24].
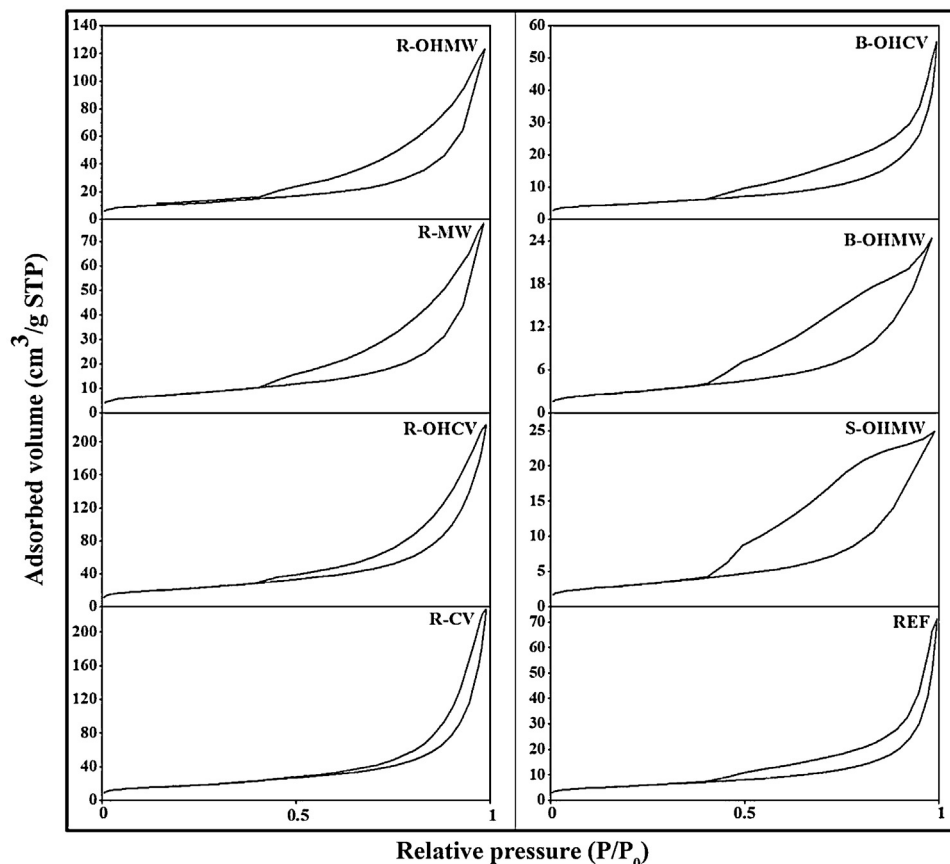

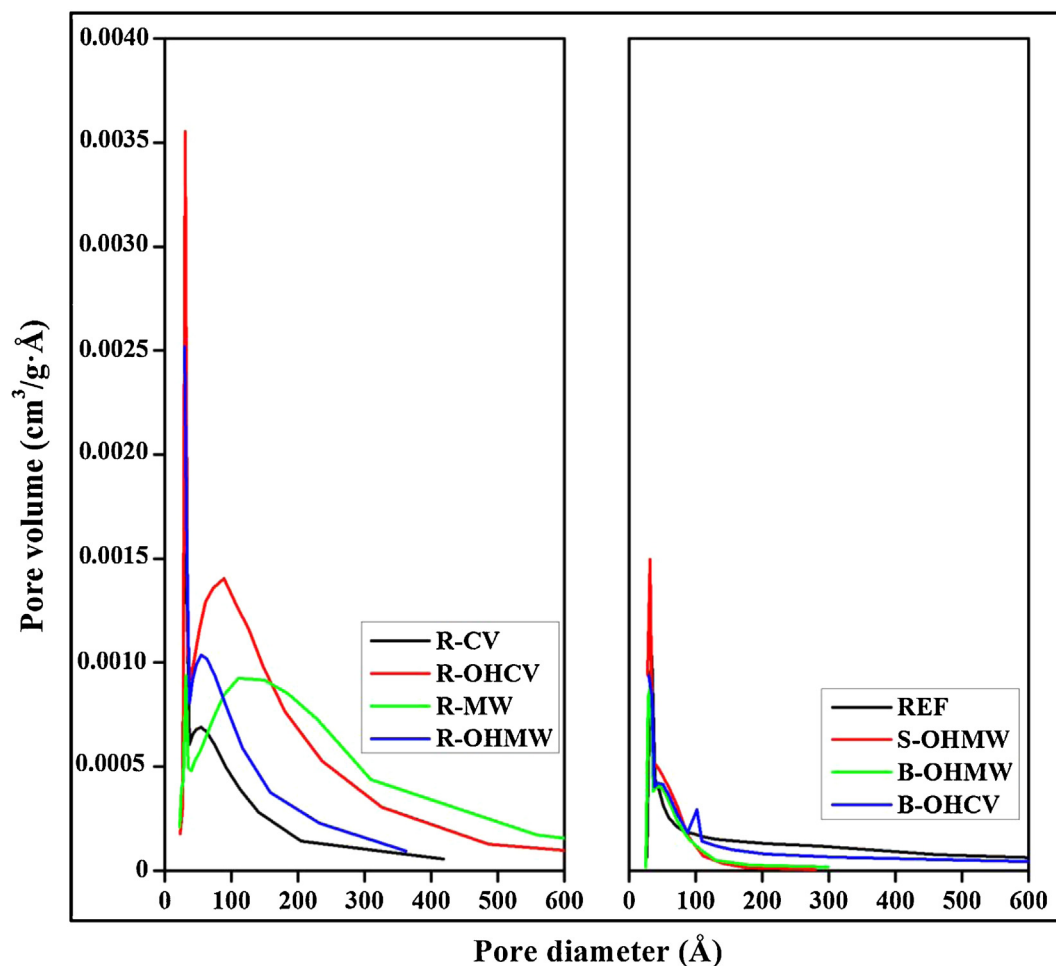**Fig. 4.** Nitrogen adsorption–desorption isotherms.

Fig. 5. Pore size distribution of the samples as determined by nitrogen adsorption.
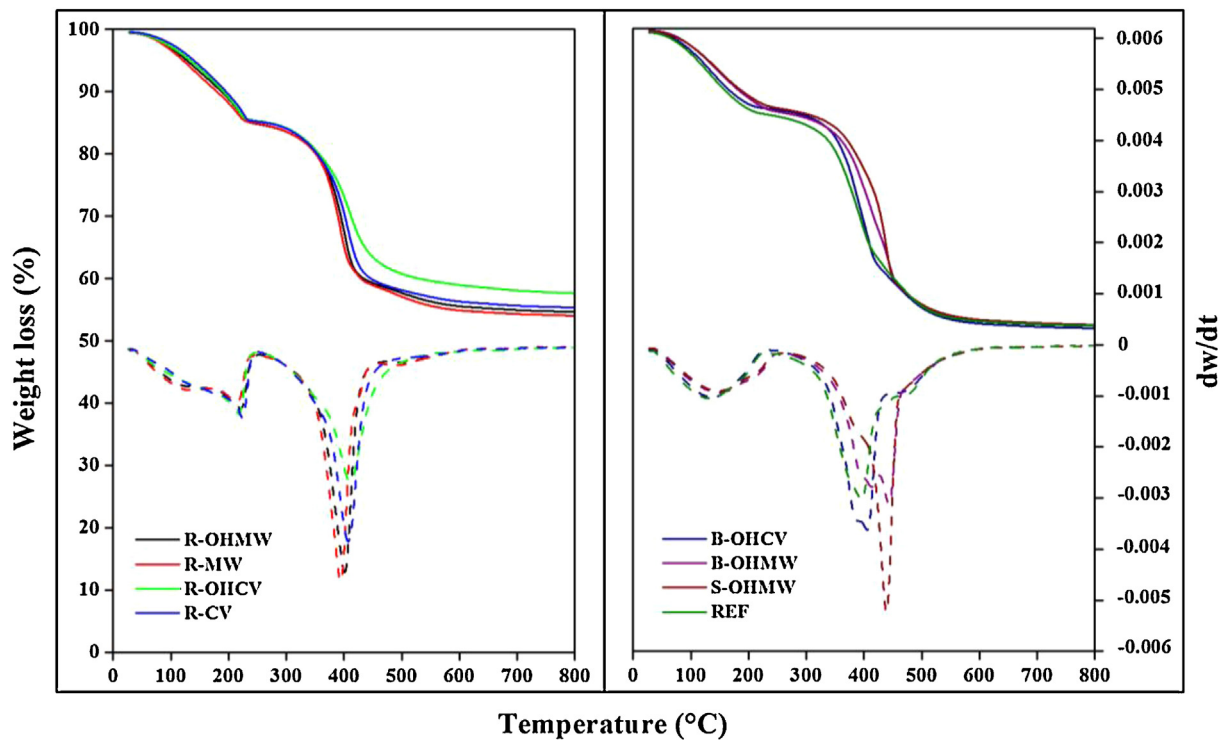

Fig. 6. TGA/DTA where weight loss corresponds to TGA curves (continuous lines) and d*w*/d*t* to DTA curves (broken lines).

Table 3
Main features of the synthesized samples.

Sample	d_{003} (Å)	Max. in pore size distr. (Å)	Pore shape	Specific surface area (m^2/g)	Green color	Thermal behavior
R-OHCV	7.7	30, 95	Slit	76	Very slight	Chlorophyllin stabilized
R-CV	7.7	30, 50	Slit	61	Very slight	Chlorophyllin stabilized
R-OHMW	7.7	30, 60	Ink bottle	39	Medium	Chlorophyllin stabilized
R-MW	7.7	30, broad peak 50–300	Ink bottle	27	Medium	Chlorophyllin stabilized
B-OHCV	8.1	30, 50	Slit	17	Slight	Cu elimination at 410 °C
B-OHMW	8.1	30, 50	Ink bottle	10	Deep	Cu elimination at 445 °C
S-OHMW	8.1	30, 50	Ink bottle	11	Deep	Cu elimination at 440 °C
REF	7.9	30, 50	Slit	20	White	

DTA curves must be a composition of both processes, Fig. 6. The profiles of exchanged samples, from 25 to 400 °C, reproduce the REF sample curve. Therefore, the peaks found at temperatures higher than 400 °C, present in the chlorophyllin containing samples and not in the REF sample, are due to chlorophyllin decomposition and desorption. The endothermal peak at *ca.* 410–445 °C, then, turns out to be due to copper elimination. Therefore, chlorophyllin is thermally more stable when it is immobilized by the hydrotalcite. As in the thermograms of regenerated samples no endothermal or exothermal peaks attributable to chlorophyllin decomposition were found, chlorophyllin is not degraded by temperature up to 800 °C.

Fig. 7. UV spectra of (a) chlorophyllin, (b) hybrids prepared by the memory effect and (c) hybrids prepared by simultaneous precipitation, compared to the reference sample REF.

3.6. UV–vis and DRS-UV spectroscopy

To provide direct evidence to confirm the presence of chlorophyllin in the host materials a characterization of the samples was made by UV–vis and DRS spectroscopy. Fig. 7 compares the spectra of pure chlorophyllin to the prepared materials. All samples reproduce the features of the chlorophyllin showing that the molecule is preserved. In the regenerated samples the peak at 625 nm is intense whereas in the samples obtained by simultaneous precipitation the same peak is faded. Reduction in absorbance at 627 nm can monitor the degradation of copper chlorophyllin complex [25]. Hence, in the simultaneous synthesis samples chlorophyllin is not as well preserved as in the memory effect prepared samples.

4. Discussion

As a general trend, all samples are crystalline hydrotalcite and no other compounds were found, the highest surface areas are provided by the syntheses by memory effect, chlorophyllin is thermally stabilized by hydrotalcite, and the microwave irradiated samples are the most colored. The present results have to be discussed depending on the preparation method, *i.e.*, using either the memory effect or the simultaneous precipitation. In each of these sections, the samples may be arranged depending on the hydrothermal treatment.

4.1. Regenerated samples

In the regenerated sample with NaOH the surface area is 76 m^2/g and the maxima of the pore size distribution are found at 30 and 95 Å. Instead, if no NaOH is used, the area is smaller (61 m^2/g) and the maxima of the pore size distribution are at 30 and 50 Å. Three ways of anchoring chlorophyllin may be advanced. Chlorophyllin may be located in the pore mouths, it may form small agglomerates on hydrotalcite or it may be intercalated between the layers. If it is anchored at the pore mouths, the surface area would be very small as N_2 cannot reach the interlamellar space. Chlorophyllin cannot be retained on the external surface forming clusters and agglomerates as chlorophyllin is an ion which cannot constitute micelles. Memory synthesis propitiates chlorophyllin intercalation in the layers of the hydrotalcite as shown by the molar ratio Cu/Al, X-ray diffraction patterns, and thermal analysis curves. This proposition is strengthened by the OH effect as the specific surface area diminishes to 61 m^2/g (sample R-CV compared to sample R-OHCV) when no NaOH is used. The OH ions are nucleating centers, therefore the number of hydrotalcite nuclei is significantly increased when NaOH is added and the obtained hydrotalcite particles are then small. When these samples are prepared in presence of microwave irradiation, samples R-OHMW and R-MW, the surface areas diminish drastically to 39 and 27 m^2/g, respectively. Again, the effect of NaOH is clear, NaOH favors a higher surface area. The X-ray diffraction interplanar distance 0 0 3 is in both cases 7.7 Å. Usually microwave irradiation increases surface area [26,27]. Bergadà et al. [28] report that a hydrotalcite aged in an autoclave by microwaves at 453 K for
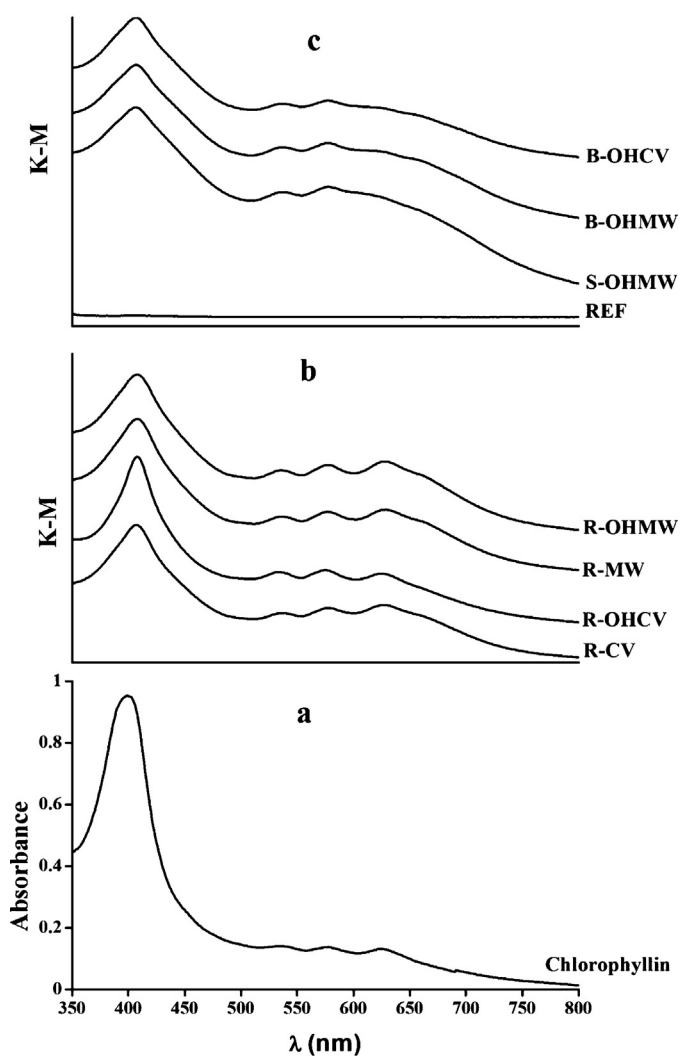
120 min shows much higher BET area and higher basicity. Furthermore, the microwave treatment leads to better crystallized LDHs with modified thermal stability and reducibility [29].

Microwave irradiation promotes, in hydrotalcite synthesis, a fast heating of the slurry avoiding thermal gradients but the inherent effect of the microwave interaction with the material cannot be excluded [29]. In our case, in presence of microwave irradiation, as the heating is homogeneous then the chlorophyllin is free to move and diffuse whereas if there were thermal gradients (conventional heating) the forces between hydrotalcite and chlorophyllin would be inhomogeneously weakened avoiding diffusion.

In the present samples, the pore size distribution presents a broad peak in the size interval from 50 to 300 Å. Such feature can only be understood if the energy provided by the microwave irradiation is excessive and disturbs the particle arrangement process, which now turns out to be more disordered forming inter-particle pores shaped as ink bottle.

4.2. Samples prepared by simultaneous precipitation

A significant difference between sample B-OHCV and the corresponding ones prepared by memory effect is the interplanar 003 distance, as in B-OHCV it turns out to be 8.1 Å. Such difference has to be explained as due to the presence of nitrates in the reaction mixture. The resulting hydrotalcite contains then carbonates as well as nitrates between the layers. Those anions are known to be preferred by the hydrotalcite. The surface area, 17 m^2/g, is slightly lower than the REF surface area, showing that chlorophyllin blocks some of the pore entrances.

When the sample is microwave irradiated, either simultaneously mixing the precursors or dropping hydrotalcite reactants onto chlorophyllin, the color is stronger, the d_{003} = 8.1 Å and the surface area drops to 10–11 m^2/g. The Cu/Al ratio shows that the amount of retained chlorophyllin is as high as in B-OHCV, but it blocks totally nitrogen access to the interlayer space. In the microwaved samples, again, the pore shape is ink bottle-like as in all other irradiated samples. Microwave irradiation then favors the anchoring of chlorophyllin and the obstruction of the pore entrances.

All samples maintained their color showing that the chlorophyllin is not oxidized or decomposed at room temperature. This point was confirmed by UV spectroscopy. Indeed, hydrotalcite is a basic solid, the functional groups are OH and they coordinate with chlorophyllin. Hydrotalcite acts as both an immobilizing medium of high mechanical strength and also as a confining environment similar to those found in biological systems. This organic hybrid may be compared with the one prepared by Murata et al. [30], where chlorophyllin is stabilized treating silica with diols. The present stabilization method is as efficient but much simpler. Furthermore, it offers the possibility to isolate chlorophyllin in different environments.

5. Conclusion

Chlorophyllin may be retained by hydrotalcite in a one step process, either by memory effect or simultaneous precipitation. Depending on the use of precipitating agent or microwave irradiation, the morphology, as well as the porosity of the samples may be controlled. Furthermore, these conditions determine the amount and location of the chlorophyllin molecules into the hydrotalcite host: between the layers or in the pore mouths. Note that microwave irradiation produces mesoporosity and small surface areas. The regeneration method promotes the intercalation of chlorophyllin.

In all cases stable materials are obtained, thus chlorophyllin molecules are isolated and bonded through hydrotalcite OH groups. Such features are required for experiments on artificial photosynthesis. The resulting compounds are non-toxic as they are constituted by chlorophyllin and hydrotalcite which is, by the way, used as stomach antiacid. Hence, it may be used as a dietary complement or simply as a food colorant.

References

[1] H.-W. Heldt, B. Piechulla, Plant Biochemistry, Elsevier, Amsterdam, 2010.
[2] B. Riemann, D. Ernst, Freshwater Biology 12 (1981) 217–223.
[3] T. Muller, M. Ulrich, K.-H. Ongania, B. Krautler, Angewandte Chemie International Edition 46 (2007) 8699–8702.
[4] T. Itoh, K. Yano, Y. Inada, Y.J. Fukishima, Journal of the American Chemical Society 124 (2002) 13437–13441.
[5] D.R. Taylor, D.B. Jenkins, C.B. Ungermann, Journal of the American Oil Chemists Society 66 (1989) 334–341.
[6] E. Gonzalez-Pradas, M. Villafranca-Sanchez, M. Socias-Viciana, A. Gallego-Campo, Journal of Chemical Technology and Biotechnology 61 (1994) 175–178.
[7] D.W. Brett, Medscape News 60 (2005) 1–7.
[8] F. Li, X. Duan, Structure and Bonding 119 (2006) 193–223.
[9] D.G. Evans, R.C.T. Slade, Structure and Bonding 119 (2006) 1–87.
[10] V. Rives, M.A. Ulibarri, Coordination Chemistry Reviews 181 (1999) 61–120.
[11] C. Aguzzi, P. Cerezo, C. Viseras, C. Caramella, Applied Clay Science 36 (2007) 22–36.
[12] C.L. Peterson, D.L. Perry, H. Masood, H. Lin, J.L. White, S.L. Hem, C. Fritsch, F. Haeusler, Pharmaceutical Research 10 (1993) 998–1004.
[13] J.A. Rivera, G. Fetter, P. Bosch, Microporous and Mesoporous Materials 89 (2006) 306–314.
[14] G. Fetter, P. Bosch, Microwave effect on clay pillaring, in: A. Gil, S.A. Korili, R. Trujillano, M.A. Vicente (Eds.), Pillared Clays and Related Catalysts, Springer, New York, 2010, pp. 1–21.
[15] E. Pretsch, P. Bühlmann, C. Affolter, Structure Determination of Organic Compounds, Springer, Zürich, 2000.
[16] F. Cavani, E. Trifiro, A. Vaccari, Catalysis Today 11 (1991) 173–301.
[17] T. López, P. Bosch, M. Asomoza, R. Gómez, E. Ramos, Materials Letters 31 (1997) 311–316.
[18] S.J. Gregg, S.W. Sing, Adsorption, Surface Area and Porosity, Academic Press, London, 1982.
[19] F. Valencia, A.H. Romero, E. Hernández, M. Terrones, H. Terrones, New Journal of Physics 5 (2003) 123.1–123.16.
[20] A. Gil, S.A. Corili, M.A. Vicente, Catalysis Reviews-Science and Engineering 50 (2008) 153–221.
[21] F. Rouquerol, J. Rouquerol, K. Sing, Adsorption by Powders and Porous Solids: Principles, Methodology and Applications, Academic Press, San Diego, 1999.
[22] A. Sampieri, G. Fetter, H. Pfeiffer, P. Bosch, Solid State Sciences 9 (2007) 394–403.
[23] M. Ishiwatari, R. Ishiwatari, H. Sakashita, T. Tatsumi, Journal of Analytical and Applied Pyrolysis 35 (1995) 237–247.
[24] T. Thanpitcha, A. Sirivat, A.M. Jamieson, R. Rujiravanit, Macromolecular Symposium 264 (2008) 168–175.
[25] M.G. Ferruzzi, S.J. Schwartz, Journal of Agricultural and Food Chemistry 53 (2005) 7098–7102.
[26] G. Fetter, A. Botello, V.H. Lara, P. Bosch, Journal of Porous Materials 8 (2001) 227–232.
[27] P. Benito, F.M. Labajos, V. Rives, Pure and Applied Chemistry 81 (2009) 1459–1471.
[28] O. Bergadà, I. Vicente, P. Salagre, Y. Cesteros, F. Medina, J.E. Sueiras, Microporous and Mesoporous Materials 101 (2007) 363–373.
[29] P. Benito, F.M. Labajos, J. Rocha, V. Rives, Microporous and Mesoporous Materials 94 (2006) 148–158.
[30] S. Murata, H. Hideo, K. Tatsuo, S. Yoshiyuki, K. Kazuyuki, Chemistry of Materials 13 (2001) 2722–2729.